



RESEARCH ARTICLE

10.1002/2018RS006540

Key Points:

- Magnetic measurements in South America ready for space weather
- Magnetic station measurement with near-observatory data quality
- New-real-time data providing proxy for Dst and the new Ksa magnetic indices

Correspondence to:

C. M. Denardini,
clezio.denardini@inpe.br

Citation:

Denardini, C. M., Chen, S. S., Resende, L. C. A., Moro, J., Bilibio, A. V., Fagundes, P. R., et al. (2018). The embrace magnetometer network for South America: First scientific results. *Radio Science*, 53, 379–393. <https://doi.org/10.1002/2018RS006540>


















Received 19 FEB 2018

Accepted 3 MAR 2018

Accepted article online 7 MAR 2018

Published online 30 MAR 2018

The Embrace Magnetometer Network for South America: First Scientific Results

C. M. Denardini¹ , S. S. Chen¹ , L. C. A. Resende¹ , J. Moro^{2,3} , A. V. Bilibio¹ , P. R. Fagundes⁴ , M. A. Gende^{5,6} , M. A. Cabrera^{7,8} , M. J. A. Bolzan⁹ , A. L. Padilha¹ , N. J. Schuch² , J. L. Hormaechea^{5,10} , L. R. Alves¹ , P. F. Barbosa Neto^{1,11} , P. A. B. Nogueira¹² , G. A. S. Picanço¹ , and T. O. Bertolotto^{1,13} 

¹National Institute for Space Research (INPE), São José dos Campos, Brazil, ²Southern Regional Space Research Center in collaboration with the LACESM/CT-UFSM, Santa Maria, Brazil, ³State Key Laboratory of Space Weather, National Space Science Center, Chinese Academy of Science, Beijing, China, ⁴Universidade do Vale do Paraíba/IP&D, São José dos Campos, Brazil, ⁵Facultad de Ciencias Astronómicas y Geofísicas, Universidad Nacional de La Plata, La Plata, Argentina, ⁶Consejo Nacional de Investigaciones Científicas y Técnicas, Buenos Aires, Argentina, ⁷Laboratorio de Telecomunicaciones, Departamento de Electricidad, Electrónica y Computación, Facultad de Ciencias Exactas y Tecnología, Universidad Nacional de Tucumán, San Miguel de Tucumán, Argentina, ⁸Centro de Investigación sobre Atmósfera Superior y Radiopropagación, Facultad Regional Tucumán, Universidad Tecnológica Nacional, San Miguel de Tucumán, Argentina, ⁹Departamento de Física, Universidade Federal de Jataí (UFJ), Jataí, Brazil, ¹⁰Estación Astronómica Rio Grande, Facultad de Ciencias Astronómicas y Geofísicas, Universidad Nacional de La Plata, Rio Grande, Argentina, ¹¹Departamento de Engenharia Elétrica, Centro Universitário Salesiano de São Paulo (Unisal-Campus São Joaquim), Lorena, Brazil, ¹²Federal Institute of Education, Science and Technology of São Paulo, Jacareí, Brazil, ¹³Departamento de Engenharia Elétrica, Universidade de Taubaté, Taubaté, Brazil

Abstract The present work is the second of a two-part paper on the Embrace Magnetometer Network. In this part, we provide some of the first scientific findings that we have already achieved with this network. We identified the diurnal and the seasonal natural variations of the H component. We provided the precise determination of sudden storm commencements and sudden impulse. We showed that the ΔH amplitudes derived from the Embrace MagNet during intense magnetic storm are in very good agreement with the Dst index. We showed that it is possible to investigate the effects on the solar quiet ionospheric current systems as a response to the X-class solar flares occurring during daytime under magnetically quiet conditions.

Plain Language Summary This manuscript is the second of a two-part paper and provides the reader with the first scientific findings from the new Embrace Magnetometer Network (Embrace MagNet), which is located in South America and is based on fluxgate magnetometer. The main purpose of this network is to fulfill the gap in magnetic measurement, which are suitable for space weather purpose. Details on the network description and its qualification are provided in the first paper.

1. Introduction

Several studies based on magnetic data have been carried out since the early researches in the field of Aeronomy with the postulation of global ionospheric current sheets (Chapman & Bartels, 1940; Lindzen & Chapman, 1969; Maeda & Kato, 1966; Matsushita, 1969; Vestine, 1960). Nowadays, it is known as the solar quiet (Sq) ionospheric current system, and it explains the global variation in ground measurements of the Earth's magnetic field that is superimposed to the main field of internal origin. Specifically with respect to low-latitude Aeronomy, Sugiura and Cain (1966) presented a model for the equatorial electrojet (EEJ) based on the horizontal magnetic component of the Earth's magnetic field (H) measured with magnetometers. Most of their work was based on the previous works made by Maynard and Cahill (1965a, 1965b). A more comprehensive study on the geomagnetic aspects of the counter electrojet was also published by Mayaud (1977) based on magnetometer measurements.

In addition to the scientific motivation, there is a growing concern to the local effects of the space weather (see definition in Denardini et al., 2016b) to the current technological assets (Schrijver et al., 2015). Some estimates from the magnetic effects of space weather lead to a global economic impact ranging from 2.4 to 3.4 trillion USD over 1 year for a major event (Schulte in den Bäumen et al., 2014). Thus, a cooperative pull of institutions, leaded by the Brazilian Study and Monitoring of Space Weather (Embrace) Program, is

installing Embrace Magnetometer Network (Embrace MagNet) in a range of approximately $50^\circ \times 40^\circ$ (latitude and longitude) in the South American sector.

The details on the instrumentation used in the Embrace MagNet, on the sensitivity matching process of the Embrace MagNet sensors, on the gain matching process for the Embrace MagNet in comparison to the Intermagnet data, and on the Embrace MagNet data quality check were provided the accompanying paper (Denardini et al., 2018) as well as in a recently publication about the research networks ready for space weather that encompasses the Embrace Magnet (Denardini et al., 2016a). In the present paper, we provide the first results we have already achieved with this network. With respect to the latter, we start presenting maps of the monthly quiet day curve (QDC) obtained at every Embrace MagNet station per the month of operation. We then discuss the response of the Embrace MagNet to the space weather drivers such as coronal mass ejection (CME, or “gas emitted during solar flares” as originally proposed by Gold, 1953) and solar wind high-speed streams (HSSs). This is done through ground magnetic measurement of sudden storm commencements (SSCs) and sudden impulses (SIs) using data collected from the Embrace MagNet. In addition, we provide some samples of the measurements made by the magnetic stations during the intense magnetic storm that occurred on 12 October 2016 and compared the evolution of the ΔH amplitudes derived from the Embrace MagNet with the Dst index. Furthermore, we investigate the capability of the Embrace MagNet to respond to X-class solar flares when they occurred during daytime under magnetically quiet conditions. Finally, to show the scientific findings that the Embrace MagNet is providing to the scientific community, we have compiled some of the recent publications that were made using the data collected by this network. However, these results presented are not discussed in details; they show the network capability.

2. Scientific Findings

In the previous part of the two-part paper on the Embrace Magnetometer Network (Denardini et al., 2018), we have showed the process applied to the whole set of Embrace MagNet network sensors in order to assure that they all have the same sensitivity to the same magnetic variation. In addition, we demonstrated that the Embrace MagNet provides data equivalent to absolute measurements, achieved after applying the proper gain matching using VSS observatory data. Thus, we were able to develop a network of magnetometer stations that provides results that are equivalent to the Intermagnet measurement (irrespective the geomagnetic conditions and season) made at magnetic observatories, which are suitable for space weather studies.

Now, we present sample of the scientific findings to illustrate the scientific capability that the Embrace MagNet is providing to the scientific community. Initially, we present examples of the magnetic measurements made by the Embrace MagNet at VSS during a quiet and a disturbed period (Figure 1). These samples are representative of the records of the Embrace MagNet measurements during magnetically quiet days and magnetically disturbed days. The left graph of Figure 1 shows the time evolution of the component of the Earth’s magnetic field registered at the VSS station on 4 December 2016, when ΣKp was 1^+ , and similar behavior was registered throughout the network (not shown here). The right graph of Figure 1 shows the time evolution of the component of the geomagnetic field during a disturbed period. For this example, we have chosen the period of 8 December 2016, when the ΣKp reached 28^- . Like the accompanying measurements, this example is also representative of the records of the Embrace MagNet measurements during magnetic disturbed days, which will be addressed ahead when comparing the evolution of the variation of the H component of the Earth’s magnetic field with the Dst index in the following sections.

Still, before going into the scientific results associated with the solar-terrestrial interaction that will be presented in the following section, we shall comment that we have three means of using the variation of the H component to for space weather studies. First, we can use it as provided by the magnetometer (Figure 4 in Denardini et al., 2018) in the final daily American Standard Code for Information Interchange (ASCII) file, that is, the variation of the H component added to its baseline value obtained from the International Geomagnetic Reference Field Model for the day of the installation. This way of using the variation of the H may be significant to those studies when it is important to show the effect observed in the magnetic measurement having the main field as a frame of reference.

Second, we may use the method of showing the variation of the H component without considering the main field, which is basically the variation of the H component deduce the baseline value or either as mentioned in the work by Denardini et al. (2009), which is reproduced in the form of equation (1):

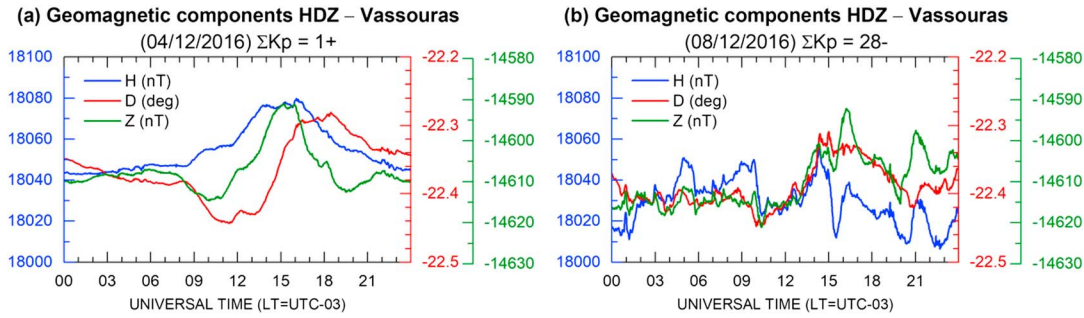


Figure 1. Time evolution of the components of the Earth’s magnetic field recorded by the Embrace MagNet instrument at the VSS station on (a) 4 December 2016 and on (b) 8 December 2016. UTC = universal time.

$$\Delta H_k(t) = H_k(t) - H_k(00 \text{ LT}), \tag{1}$$

in which “*t*” is the time (from 00 h00 to 23 h59 UT with 1 min time resolution), “*k*” is the magnetic station code (station numbers 1, 2, 3, and so forth), *H*(*t*) is the daily variation of the horizontal component, and 00 LT corresponds to the local midnight at the magnetic station. This method will show the behavior of the *H* component considering both the local (atmospheric or solar radiation) and external (solar wind) forcing.

The third way of obtaining the variation of the *H* component, which is also suitable for space weather studies, is defining ΔH according to equation (2):

$$\Delta H_N(t) = \frac{1}{N} \sum_{k=1}^N [H_k(t) - \text{QDC}_k(t)], \tag{2}$$

in which *t*, *k*, and *H*(*t*) are the same as defined in equation (1), while *N* is the number of magnetic station comprised in the derivation is the daily variation of the horizontal component. QDC(*t*) is the daily variation of the monthly averaged horizontal component, acquired during the five quietest days of the month (Denardini et al., 2015). This method will select the *H* component considering only external (solar wind) forcing once the local forcing (atmospheric or solar radiation) were removed by subtracting the QDC, which will be addressed in the next section.

2.1. Diurnal Variation of Monthly QDC Measured at the Embrace MagNet Stations

In this section, we present the results regarding the daily variation of the monthly QDC. The scientific motivation for working on the determination of this for each Embrace MagNet stations is mainly due to its need for the determination the Ksa index, which is currently under development. Furthermore, through the QDC we are able to identify and study the diurnal and seasonal variation of the magnetic field that may lead to the development of a complementary model to the International Geomagnetic Reference Field. Such models might provide additional information on the variation of the field due to the Sq over South America. This motivation follows the spirit of developing the magnetic models, which include the diurnal and seasonal variation, as per example but not limited to those listed in Table 1.

However, the task of determining the QDC—usually thought to be simple—is quite complicated in the Southern American sector. The magnetic declination at low latitudes in the Brazilian sector (eastern portion of South America) reaches -20° . Consequently, the westward drift of the main magnetic field (associated with the secular variation) provides deviation with the almost decadal scale at this longitude. Thus, the QDC can drastically change within few years’ period. See, for instance, the difference between the average diurnal evolutions of the ΔH component of the Earth’s magnetic field registered around summer at the SLZ in 2002 and 2012, which are shown in Figure 2.

The average diurnal evolution of the ΔH component (summer QDCs for simplification) registered in the graphs of Figure 2 was obtained by averaging the entire set of daily ΔH obtained for *H* component measured by the ground magnetometers during the summer in the Southern Hemisphere using equation (1). The error bars represent one standard deviation of the daily ΔH with respect to the summer QDC. The upper panels of this figure show the summer QDC registered at the SLZ station (red dots) and at the EUS station (blue dots). The bottom panels show the differences between the summer QDC for SLZ (an equatorial station in 2002)

Table 1

List of Magnetic Field Models, Accompanied by Their Respective References, Which Are Able to Provide the Seasonal and Daily Variation of the Earth's Magnetic Field to Some Level

Reference	Basic description of the model
Sutcliffe (1999)	Empirical model developed for providing a geomagnetic daily variation over the Southern African region as a function of season, sunspot number, and degree of geomagnetic activity, based on artificial neural networks
Alken and Maus (2007)	Empirical model of the equatorial electrojet magnetic signature as a function of longitude, local time, season, solar flux, and lunar local time, derived from CHAMP, Ørsted, and SAC-C satellites
Unnikrishnan (2012)	Empirical model for providing a geomagnetic daily variation over the Alibag observatory, India, for solar quiet conditions, based on artificial neural networks
Oquadfeul et al. (2015)	Empirical model for providing a geomagnetic daily variation over the German Wingst observatory, Germany, as function of degree of geomagnetic activity, based on artificial neural networks
Jayapal et al. (2016)	Empirical model developed for the horizontal component of the Earth's magnetic field over Thiruvananthapuram, India, as a function of the solar cycle, seasonal, and degree of geomagnetic activity, based on Fourier analyzes

and EUS (a low-latitude station close to the dip equator in 2002), which provides the magnetic signature of the EEJ at the ground level (black dots). Above the panels we present the averaged sunspot number (SSN) corresponding to the period covered by the data in the graphs.

Comparing the amplitudes of the summer QDC at EUS in 2002 with those measured in 2012, one may infer that solar activity may influence the amplitude of the Sq system. The maximum values of this QDC decreased from around to 95 nT (at SSN 104.0) in 2002 to little more than 50 nT (at SSN 57.7) in 2012, which is 47% decrease in the field (even considering the standard deviation) for a 44% solar activity reduction, although, in the same time period, summer QDC at SLZ reduced from 175 nT to around 60 nT, that is, 65%. Therefore, the changes in the solar activities cannot completely explain the entire decrease in the daily variation over these two regions. Assuming that the changes in the solar activities will affect homogeneously all the station that are close apart (like these two), we may infer that the measurement made at the SLZ station registered the strong influence of the EEJ in the first period of data and practically no influence in the second period of analysis, due to the westward drift of the main magnetic field.

This result provides evidence that SLZ is no longer an equatorial station since circa 2012. In addition, since the data collected by the Embrace MagNet aimed to be used for deriving the Ksa index, it also means that another approach besides the "conversion table subdivided by seasonal" for each station shall be considered when standardizing the K index measured at each individual magnetic station before average them

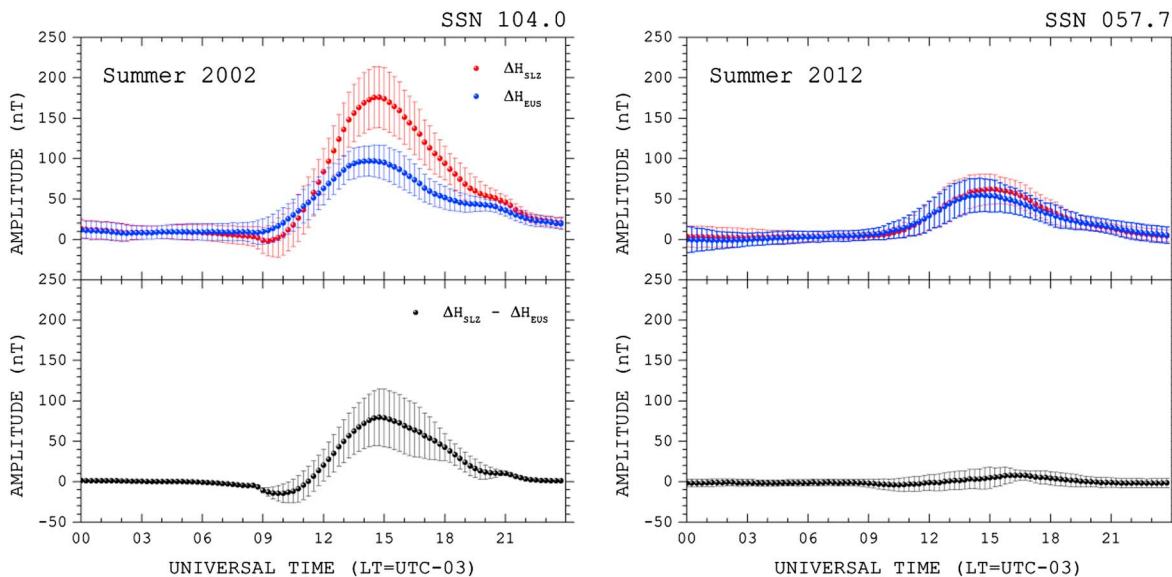


Figure 2. Average diurnal evolution of the ΔH component of the Earth's magnetic field registered at the SLZ station (red dots), the EUS station (blue dots), and the difference between them (black dots) for the summer of 2002 (left graphs) and summer of 2012 (right graphs). SSN = sunspot number; UTC = universal time.

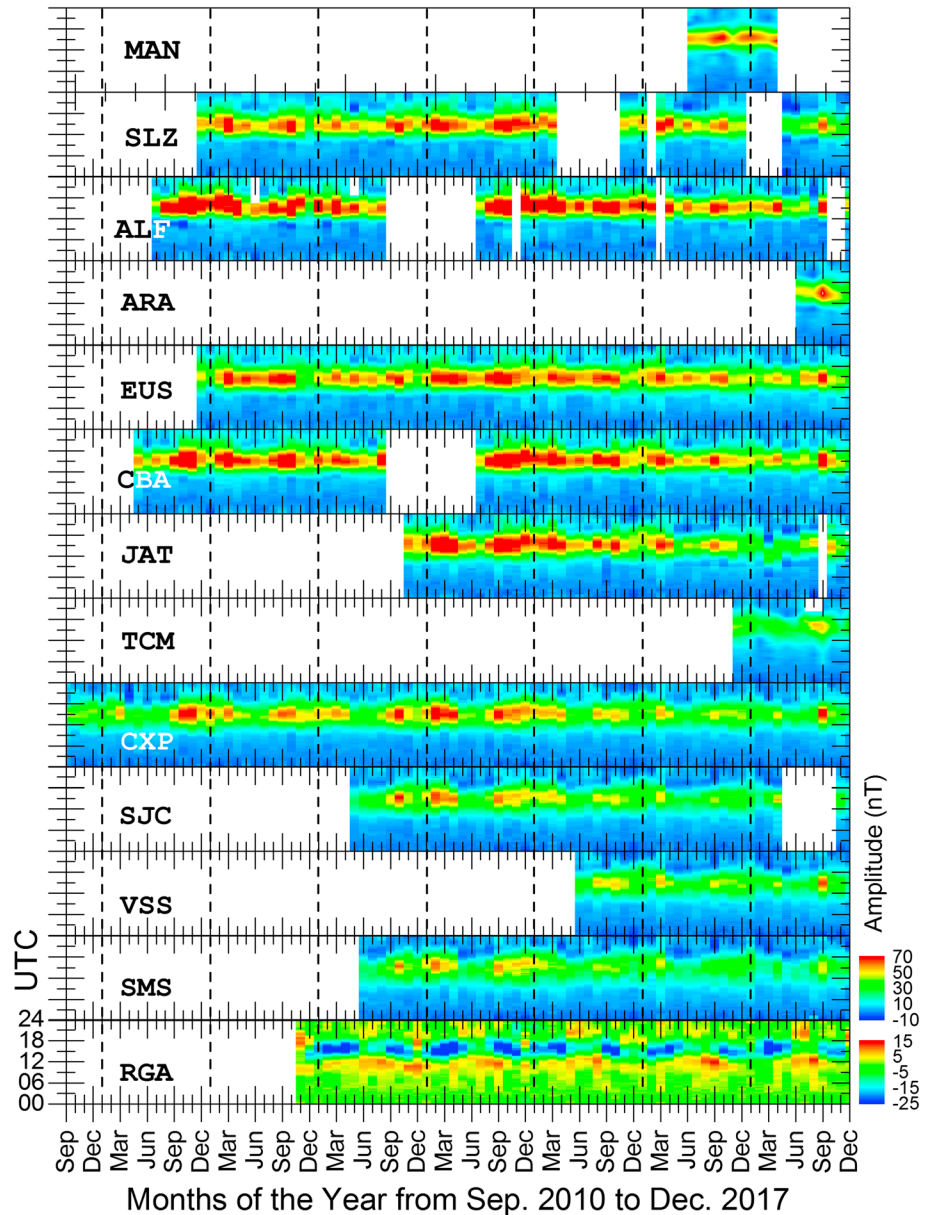


Figure 3. Monthly quiet day curve (QDC) color maps for the H component of the Earth's magnetic field from September 2010 to March 2016 at 10 Embrace MagNet stations identified in the bottom left side of each map. UTC = universal time.

(Rostoker, 1972). Therefore, we decided to investigate the use of equation (2) for computing the range of the component over the 3 h period at each magnetic station ($N = 1$) instead of using the H variation (or either X and Y components) given by equation (1). This approach leads to the need to build the monthly QDC for each Embrace MagNet station, whose annual evolution are presented in the maps of Figure 3.

The 13 colored maps of Figure 3 show the evolution of the QDC for the H component of the Earth's magnetic field measured from September 2010 to December 2017 at 13 Embrace MagNet stations identified in the bottom left side of each map. Each column of the maps corresponds to the diurnal variation of the monthly QDC for the corresponding magnetic station and is referred to the universal time as presented in the vertical axis of the bottom map. The month of the year, which the QDC is referred to, is presented in the horizontal axis of the bottom map. The color scales provide the amplitudes of the monthly QDC, ranging from -10 to $+70$ nT in all cases, except for RGA that ranges from -25 to $+15$ nT. The vertical dashed lines identify the beginning of the years. Therefore, the maps are organized in a way that we can identify the evolution of

value of the QDC (given by the color scale) at a given universal time (vertical axis) with respect the months of the year (horizontal axis).

From these maps, we are able to identify easily 2 out of the 10 natural variations of the H component described by Samson (1991): the diurnal and the seasonal variations. Essentially, the diurnal variation is a manifestation of the well-known Sq, which is characterized by the increasing (decreasing) of the horizontal field for those station located between (outside) the foci of the Sq current system during the morning hours and the opposite in the evening hours, being close to baseline during nighttime. The behavior for the stations between the foci of the Sq current system is evident in all the maps of Figure 3, except for the RGA station that seems to be close to—or a bit southern than—the southern hemispheric focus. The seasonal variation also pops out from these maps. Independent of the Embrace MagNet station, one can clearly recognize that there is a seasonal pattern marked by one or more annual peaks of intensity in the monthly QDCs. Taking CXP as an example, it is possible to see that the QDC peaks around summer in the Southern Hemisphere (December–January). Thus, these natural variations are another topic for further investigations.

2.2. Response of the Embrace MagNet to the Space Weather Drivers

Among the space weather forcing that impact the Earth’s magnetosphere system, we have the arrival of the CME and the solar wind HSS. The former is associated with the solar bursts, and the latter are associated with coronal holes on the solar corona. Those solar phenomena are known for having remarkable signatures in the measurements made outside the magnetosphere (Allen, 1944; Gonzalez et al., 1994; Gopalswamy, 2016; Gopalswamy et al., 2009; Obayashi, 1964; Wilson et al., 2007) as well as for producing clear sudden effects on magnetic measurements at the ground level (Araki, 1994; Curto et al., 2007; Gold, 1962; Matsushita, 1962; Shinbori et al., 2010). The explanation for these magnetic records came with the early work published by Schutz et al. (1974). They stated that geomagnetic SI generated hydromagnetic waves that propagate toward the Earth through the plasma of the magnetosphere. Among their results, they have shown that electric fields are generated in the Earth’s ionosphere due to its interaction with the hydromagnetic waves. Consequently, these electric fields drive ionospheric currents, which are detected by ground-based magnetometers as sudden increase in the H component of the geomagnetic field. These are the currently well-known SSC or SI. Based on this knowledge, we provide ahead the first results obtained from data collected by the Embrace MagNet with respect to the response of magnetic measurement at ground level to SSC and SI.

For the present manuscript, we selected only two cases, which are representative of the capability that the Embrace MagNet data can provide. The first example is the case of the SSC registered on 8 March 2012, and the second one is a SI registered on 21 May 2012, few days after the first event. In both cases, we present the individual variation of magnetic H component collected at ALF, CBA, CXP, EUS, and SLZ, obtained by using equation (2) ($N = 1$) covering the period before and after the SSC and SI but not the whole disturbed period. Along with these data, we included the variation of the interplanetary magnetic field (IMF) B_z and the solar wind dynamic pressure (P_{sw}) provided by the Global Geospace Science Wind satellite at the L1 Lagrangian point. The IMF B_z is a direct measurement of the IMF made by the Magnetic Field Instrument that is composed of dual triaxial fluxgate magnetometers (Lepping et al., 1995) on board Wind. The P_{sw} is the kinetic energy per volume unit of the solar wind, and it is a function of wind speed and its density. It is calculated by equation (3):

$$P_{sw} = 1.6726 \times 10^{-6} \cdot n_e \cdot V_{sw}^2, \quad (3)$$

in which “ P_{sw} ” is the solar wind dynamic pressure given in nanopascal (nPa), “ n_e ” is the solar wind plasma density given in particles per cubic centimeter (cm^{-3}), and “ V_{sw} ” is solar wind speed given in kilometer per second (km/s). All these variables are also measured on board Wind (Gloeckler et al., 1995; Ogilvie et al., 1995).

2.2.1. SSC Registered on 8 March 2012

The example of the SSC case registered on 8 March 2012 is presented in the graphs of Figure 4, where we show the time variation of (from the top to the bottom) the IMF B_z , the P_{sw} , and the magnetic ΔH component collected at the five Embrace MagNet stations, individually. The different colors of the lines in the bottom graph identify from which magnetic station the magnetic H component comes. The vertical dashed line identifies the time of occurrence of the SSC, whose precise information appears on the upper left corner of the upper graph obtained from the International Service of Geomagnetic Indices (ISGI) website.

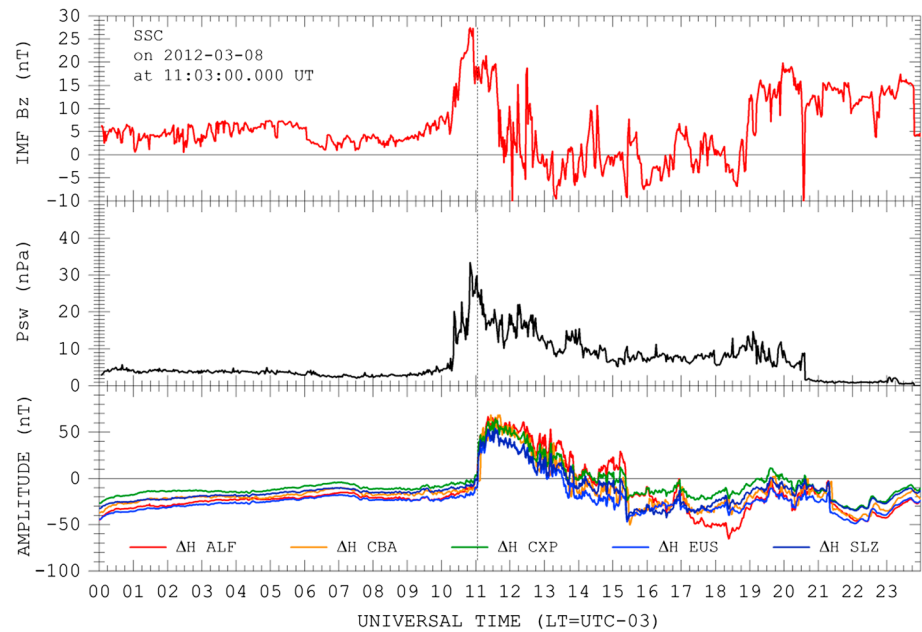


Figure 4. Time evolution of the (upper) interplanetary magnetic field (IMF) Bz, (middle) solar wind dynamic pressure, and (bottom) individual variation of magnetic ΔH component collected at ALF, CBA, CXP, EUS, and SLZ on 8 March 2012. SSC = sudden storm commencements. UTC = universal time.

In the present case, a CME hits the Earth on 8 March 2012 and was produced by the solar active region (AR) identified as AR 1429, after the X1.3 solar flare occurred at roughly 01:00 UT on 7 March 2012 (Tsurutani et al., 2014). The Kp magnetic index registered 5 at the moment of the SSC, while the Dst index recorded -27 nT. The time evolution of the IMF Bz shown in Figure 4 demonstrates that the interplanetary shock driven by a CME started to pile up the field lines at around 08:45 UT, which rose the IMF Bz from about 5 nT to more than 25 nT minutes before the SSC to be registered at the ground level. After the manifestation of the shock in the IMF Bz, the P_{sw} registered a sharp increase in just 8 min changing from 4.6 nPa at 10:14 UT to more than 20 nPa at 10:22 UT. This increase was followed by fluctuation that lead the pressure to peak in 33.3 nPa at 10:50 UT, 13 min before the clear manifestation of the magnetic storm SSC at 11:03 UT, which was also registered by the five stations that are part of the Embrace MagNet at the same time (bottom panel of Figure 4). Consequently, we can conclude that time of the SSC as measured by the H component on the Embrace MagNet matches with the SSC precise information revealed by the ISGI and it is consistent with the order of increases in IMF Bz and P_{sw} as well of time lag between events.

Finally, it is important to mention that we did not perform the analysis of the amplitude of the SSC recorder by our data with respect to the theory proposed by Siscoe et al. (1968) and applied by Ogilvie et al. (1968), which stated that the amplitudes of the SSC are roughly proportional to the square root of the solar wind dynamic pressure changes. Additionally, we did not discuss here the type of the SSC we observed, as per the original classification proposed by Matsushita (1962) that classifies the SSC in different types as well as presents their local time and latitudinal dependences. Moreover, we have not discussed the observational aspects of SSC, such as the morphology (Araki, 1994; Curto et al., 2007). All these points are to be addressed in a specific study that is currently under development. The present paper only focused in showing the magnetic measurements made by the Embrace MagNet.

2.2.2. SI Registered on 21 May 2012

The example of the SI case registered on 21 May 2012 is presented in the graphs of Figure 5 in the same way as the preceding figure with the SSC event. It shows the time variation of (from the top to the bottom) the IMF Bz, the P_{sw} and the magnetic H component collected at the five Embrace MagNet stations, individually. In addition, the different colors of the lines in the bottom graph identify from which magnetic station the magnetic H component comes. The vertical dashed line identifies the time of occurrence of the SI, whose precise information appears on the upper left corner of the upper graph (also from the ISGI).

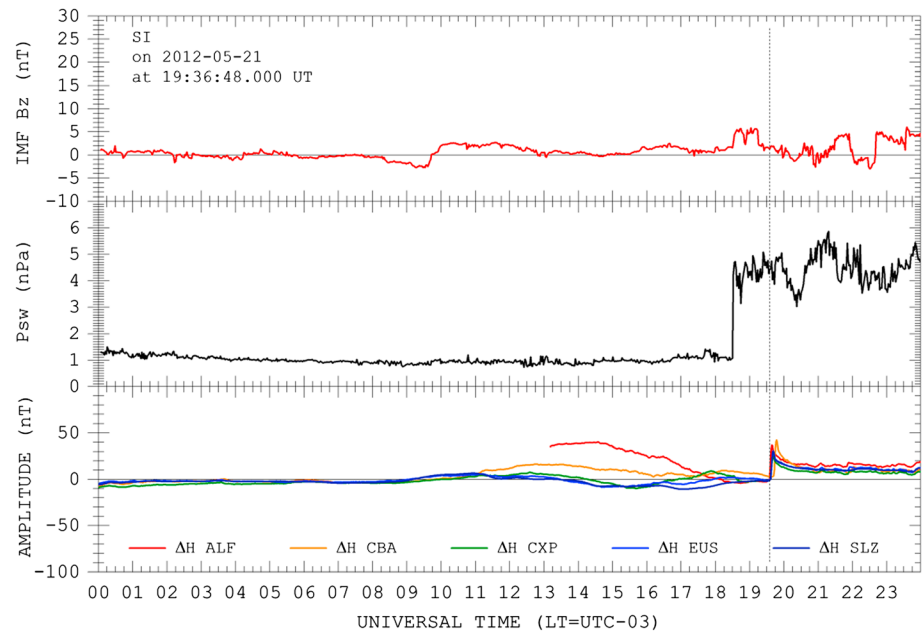


Figure 5. Time evolution of the (upper) interplanetary magnetic field (IMF) Bz, (middle) solar wind dynamic pressure, and (bottom) individual variation of magnetic ΔH component collected at ALF, CBA, CXP, EUS, and SLZ on 21 May 2012. SI = sudden impulse; UTC = universal time.

The SI chosen to exemplify the capability of the Embrace MagNet was enrolled in the study published by Samsonov et al. (2014) along with several other cases that they observed with the Time History of Events and Macroscale Interactions during Substorms spacecraft. According to information on their Table 1, the SI occurred at 19:37 UT, while the Dst registered 10 nT. They also stated that the magnitude of the magnetic compression of this particular event was the smallest recorder one among the events they analyzed. In addition, the velocity oscillations associated with this event presented slightly different behavior when compared to seven other SIs listed in the study. Irrespective these peculiarities, the magnetospheric magnetic field showed fluctuations (especially after 09 UT) that were followed by the jump in the solar wind dynamic pressure before the SI, as expected. The P_{sw} rose up from 1 nPa at 18:29 UT to 4.2 at 18:31 UT. Thereafter, the magnetometers of the Embrace MagNet (bottom panel of Figure 5) recorded the jump at the ground level 68 min later, that is, at 19:37 UT, which matches with the SI information resealed by the ISGI, as in the SSC case.

With respect to the causative effect of this SI, it is well known that SIs have been proved to be caused by the same physical mechanisms as SSCs, which is the dynamic pressure increase that compresses the Earth's magnetosphere. However, SIs are not followed by a magnetic storm (Curto et al., 2007). This is the case for the present event (not shown here). The IMF Bz does not show any evidence of the interplanetary CME signature. Consequently, we attribute the SI shown in the example of Figure 5 to the HSS arriving from the recurrent coronal hole that was passing close to the solar central meridian at this time. Supporting the hypothesis of the HSS coming from the coronal hole, we observe that the jump in the P_{sw} was followed by oscillations that are known to be associated with the shock. Such oscillations far from the Sun are known since the 1970s as Alfvén waves. They were suggested as possible source of heating that accelerates the solar wind and to some extent that the low-frequency Alfvén waves can be a significant source of heating of coronal holes at several solar radii (Ofman & Davila, 1995). Recently, Morton et al. (2015) have demonstrated that counterpropagating Alfvénic waves also exist in open coronal magnetic fields. They further stated that these waves reveal key observational insights into the details of their generation, reflection in the upper atmosphere, and outward propagation into the solar wind.

In any case, we did not provide full evidence that this SI is due to the HSS coming from the coronal hole once this is not the purpose of the present analysis. We aim to prove the capability of the magnetic measurements made by the Embrace MagNet for space weather studies, which we believe to be the case from the jump recorded by all the magnetometers of the Embrace MagNet 68 min after this small-amplitude SI to be

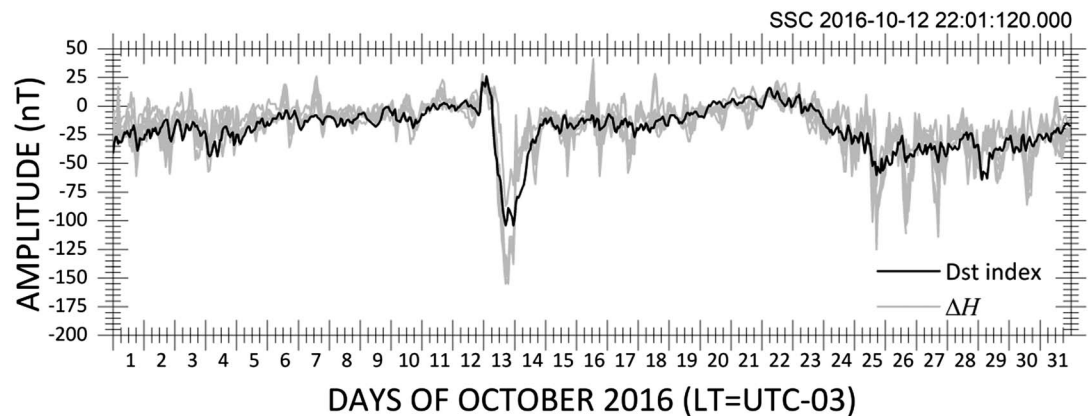


Figure 6. Variation of the (black line) Dst index for the days of October 2016 and the (gray lines) measurements of the variation of the deviation of the H component with respect to the quiet day curve for all the Embrace MagNet stations available for the same period. UTC = universal time.

recorder at L1. Moreover, all these highlighted hypothesis and details on the interpretation of this data are to be addressed in a specific study that is currently under development.

2.3. Magnetic Storms Registered on 12 October 2016

In addition to the response of the Embrace MagNet to the SSC and SI, we now provide a sample of the measurements made by the magnetic station during the intense magnetic storm ($Dst = -104$ nT) occurred on 12 October 2016. Figure 6 shows the variation of the (black line) Dst index for the days of October 2016 along with the (gray lines) measurements of the variation of the deviation of the individual H component (as derived by equation (2)) for all the Embrace MagNet stations available for the same period.

The morphology of geomagnetic storms has been studied by various researchers, such as the pioneer's works published by Chapman and Bartels (1940) and Vestine et al. (1947), the review work published by Matsushita (1962), and the most recent review published by Gonzalez et al. (1994). However, as the scientific findings presented in the previous sections, we will not explore the present results to all its extent. A comprehensive analysis to investigate the response of the evolution of ΔH derived from the Embrace MagNet throughout the Saint Patrick's Day geomagnetic storm as compared to the evolution of the Dst index is being submitted for publication soon. There we compared the ΔH for the Embrace MagNet network to the evolution of the Dst index, compared the ΔH considering a different number of Embrace MagNet station comprised in its derivation to the evolution of the Dst index, and compared the ΔH for some selected Intermagnet observatories to the evolution of the Dst index to verify the application of our methodology for deriving the ΔH .

Thus, from the simple example, we show that the available Embrace MagNet stations presented a coherent response to the presence of the magnetic disturbance. All the stations recorded the deviation of the H component with respect to the QDC in the same way and at the same time. Additionally, all the stations were able to reproduce the temporal evolution of the Dst index, which is designed to provide an evaluation of the magnetospheric ring current. Nevertheless, it is important to note that there are some discrepancies with respect to the amplitudes of the measurements with the Dst during the magnetic storm, when it registered its minimum values like at 17 UT on 13 October 2016. At this moment, $Dst = -104$ nT while the low-latitude stations (from the equator to outward it) registered $\Delta H_{MAN} = -130$ nT, $\Delta H_{ALF} = -143$ nT, $\Delta H_{EUS} = -130$ nT, $\Delta H_{CXP} = -141$ nT, $\Delta H_{SJC} = -144$ nT, and $\Delta H_{SMS} = -149$ nT. The only station that registered values lower than the Dst was the middle latitude one, located at RGA where the $\Delta H_{RGA} = -87$ nT.

At this point, we shall recall the attention of the reader that we have not applied any latitudinal correction to the magnetic data from the Embrace MagNet stations. This subject is stressed here because we would like to highlight the fact that even with no magnetic correction, the Embrace MagNet station situated under the SAMA, that is, SMS, registered the highest variation of the H component. Moreover, the entire stations recorded values slightly higher than the Dst index. Considering the fact that the magnetic observatories whose data are used for deriving the Dst are set in latitudes higher than our station; this result is not

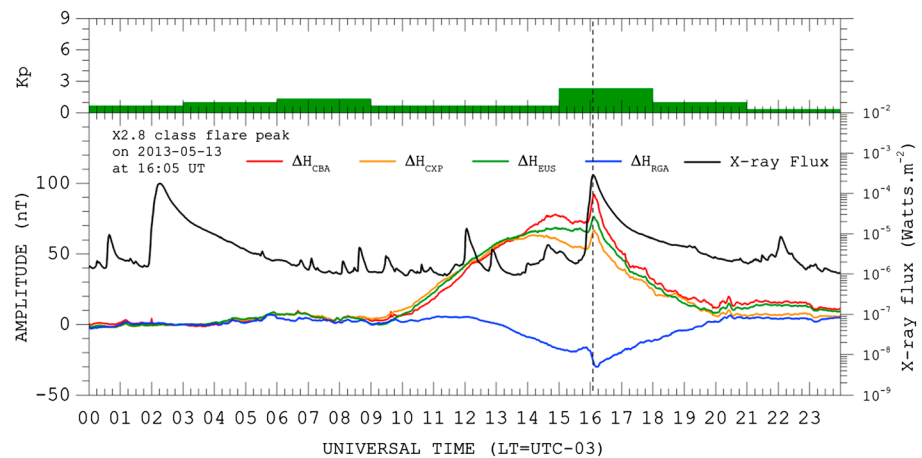


Figure 7. Diurnal variation of (upper) the Kp index, (bottom) the individual variation of magnetic ΔH component collected at CBA, CXP, EUS, and RGA, and the X-ray flux in the range of 1–8 Å, on 13 May 2013. UTC = universal time.

surprising. Finally, since RGA is set far from the magnetic equator, we also expected it to register lower values. In conclusion, there is an excellent agreement with respect to the timing of the magnetic storm and to the evolution of its phases. Furthermore, there is a quite good agreement among the amplitudes, despite the low-latitude stations of the South American sector registered a little higher value.

2.4. Flares and the Effects Measured by the Embrace MagNet

Another scientific finding we would like to present to exemplify the capability of the Embrace MagNet is the response of the network to X-class (above 10^{-4} W/m^2) solar flares when they occurred during daytime under magnetically quiet conditions ($Kp \leq 3^+$). In Figure 7, we show the diurnal variation of the Kp index (obtained from the World Data Center at Kyoto, Japan) on 13 May 2013 in the top panel. The bottom panel of the same figure shows the ΔH component individually collected at the four Embrace MagNet stations for the same period (calculated using equation (1)). Superimposed to these ΔH variations, we have the time variation of the X-ray flux in the range of 1–8 Å, measured at the Geostationary Operational Environmental Satellite 15, which is located at 135°W over the Pacific Ocean. The different colors of the lines in the bottom graph identify the magnetic station corresponding to the magnetic H component and the X-ray measurement. The vertical dashed line identifies the time of occurrence of the solar X2.8 flare, whose precise information appears on the upper left corner of the upper graph.

This diurnal variation of the X-ray flux shows the occurrence of two X-class solar flares. Both flares occurred during magnetically quiet conditions, as confirmed by the Kp index in the top panel of Figure 7. The first occurred at 02:17 UT, which means that the American sector (roughly UT-2 to UT-5) was in the nightside of the Earth. The second X-class flare occurred from 15:48 UT to 16:16 UT, peaking at 16:05 UT. This means that the whole Embrace MagNet was registering magnetic variation close to midday (UT-3 in Brazil). The results showed that low-latitude stations (CBA, CXP, and EUS) presented a sudden positive disturbance in the ΔH variation, while the midlatitude station (RGA) offered a negative disturbance in its H component. These sudden disturbances (positive and negative) started at 15:54 UT, however. In all the cases, we can identify extremely small amplitude oscillations in the ΔH variation measured in all the stations, and it seems to happen coherently in time.

Indeed, Nogueira et al. (2015) studied the X-class flare event along with total electron content data, ionosonde data, and some additional magnetic measurements. They did not mention the small-amplitude oscillations in the ΔH variation measured in all the stations after the solar flare occurrence. However, they stated that the positive response in ΔH at low latitude with its simultaneous negative response at the midlatitude station is a clear demonstration that the solar flare additional ionization causes strong enhancement in the entire Sq current system. In addition, we would like to comment that this simultaneous increment might be used to identify the distance of the corresponding station to the focus of the Sq, which we estimate to be almost equidistant of CXP and RGA.

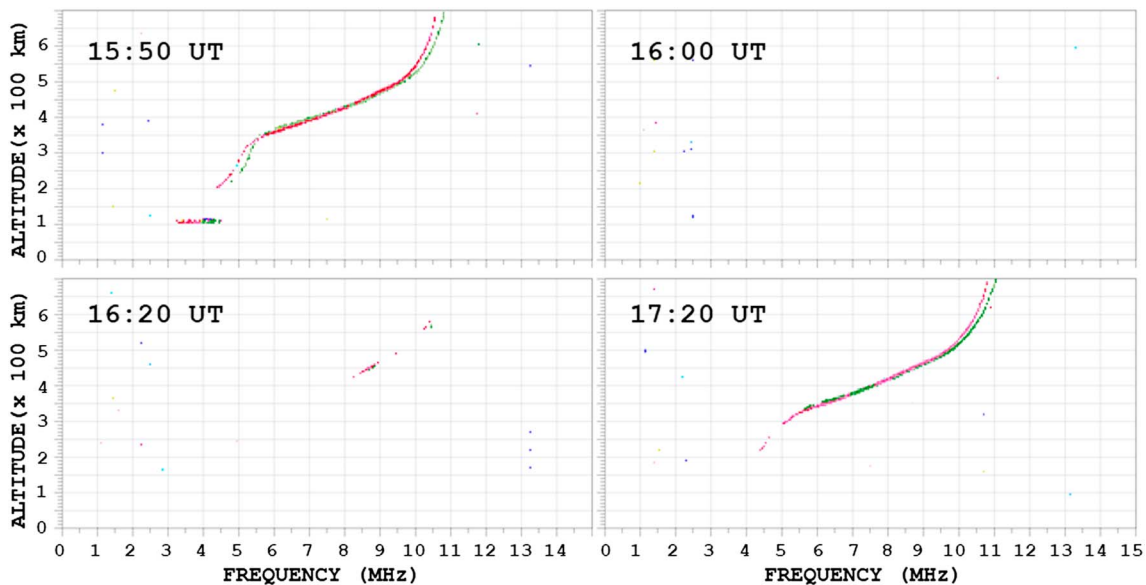


Figure 8. Sample of ionograms recorded at SLZ at four different moments around the X2.8 flare occurred on 13 May 2013.

Finally, in order to reinforce the influence of the manifestation of the additional ionization due to the solar flare, we present Figure 8 that shows sample of ionograms (usually taken in intervals of 10 min) recorded at SLZ at four different moments around the X2.8 flare that occurred on 13 May 2013. It is well known that the extreme ultraviolet with wavelengths ranging from 1,027 to 1,118 Å is responsible for the ionization of the minor constituents present at the *D* region heights, while the X-ray solar radiation (with wavelengths between 2 and 8 Å) is responsible for the ionization of all the atmospheric constituents. Indeed, Thomson et al. (2004) stated that an increase in the X-ray flux to a level of only 10^{-6} W/m² has a just detectable effect on the *D* region of the ionosphere. Therefore, the additional radiation from this X2.8 solar flare certainly increased the *D* region density. Consequently, it would lead to an increase in its opacity to shorter wavelength electromagnetic (EM) signals propagating upward (Denardini, Resende, et al., 2016). Such opacity will appear in the ionograms as a blackout of the sounding waves having shorter wavelengths (few megahertz). This is the present case of the four ionograms of Figure 8.

The ionogram corresponding to the soundings at 15:50 UT shows the typical ordinary (green pixels) and extraordinary (red pixels) traces of the *E* and *F* regions (including the sporadic *E* at around 100 km height). Here it is important to mention that, despite the solar flare have been started at 15:48 UT, the X-ray flux at this time seems not to have reached the lowest threshold, which would increase the density to the level of blocking the shorter wavelength EM waves. The first manifestation of the ionospheric density increase is only seen by the ionosonde at 16 UT. However, as mentioned above, the 6 min lag time between the flare and the sudden disturbances in ΔH variation measured in all the stations suggests that the Sq system was already experiencing the solar flare manifestation at 15:54 UT.

The ionospheric recovery phase seems the start at 16:20 UT, as per the ionogram observations. The soundings made at this moment start to display the upper *F* region (around 450 km height), meaning that the lower ionosphere was no longer opaque to the EM waves with frequencies higher than 8 MHz. When looking back at the ΔH variation measured at this moment, they all seemed to correspond to the ordinary ΔH variation, which supports the ionospheric observation. The complete ionospheric recovery seems to have finished at 17:20 UT, when the full ionospheric traces come up to the ionograms again.

Thus, the record of the electron density presented through the ionograms corroborates to show that the measurements made by the Embrace MagNet might provide responses to X-class solar flares occurring during daytime under magnetically quiet conditions. The set of ionograms showed the blackout of the shorter wavelengths EM waves as a response to the sudden ionospheric density increase, while the ΔH variation measured in all the stations revealed a positive response in ΔH at low-latitude and a negative response at

the midlatitude station, simultaneously. In addition, the Embrace MagNet measurements exhibited small-amplitude oscillations after the occurrence of the solar flare.

2.5. Recent Publication Based On the Data Collected by the Embrace MagNet

Finally, in order to complement the scientific finds that the Embrace MagNet is proving to the community, we compile in this section some of the recent publications, which were made by using the data collected by this network. We will not rediscuss the results presented by the original authors though. They were included here to exemplify the capability of the network only.

The first set of scientific findings we would like to mention deals with the use of magnetic data to support the ionospheric studies. Santos et al. (2016) used the magnetic data to complement the smoothed vertical drift of the ionospheric *F* region over Fortaleza. In this case, the magnetometer data were used for determining the vertical drift of the ionosphere during the daytime, while the Digisonde data were used for the nighttime.

In some other cases, the magnetic data collected by Embrace MagNet were used to support the study of the coupling between the neutral atmosphere and the ionosphere, as in the publication by de Jesus et al. (2017) during the 2012 minor sudden stratospheric warming. Among the results, they used the ground-based magnetometer measurements in the American sector to show strongly enhanced EEJ after the sudden stratospheric warming temperature peak. Still on ionospheric studies but now related with the EEJ, the magnetic data collected by the Embrace MagNet were used to show the EEJ day-to-day variability and its role on the day-to-day characteristics of the equatorial ionization anomaly over the Brazilian sector as compared to the Indian sector (Venkatesh et al., 2015). In this case, it was used along with and compared to vertical total electron content information.

The second set of scientific findings, which is related to our magnetic measurement in South America, deals with seismology and electromagnetically induced ground currents. Klausner et al. (2017) presented the first report on seismogenic magnetic disturbances over the Brazilian sector. The study was based on data collected at seven low-latitude Embrace MagNet stations (see their Table 1) that registered the magnetic effects of the Illapel earthquake, occurred on 16–17 September 2015. According to these authors, the magnetometers (distributed within 4,500 km from the epicenter) detected the presence of magnetic disturbances around 15 min after the earthquake. They also included an analysis of the seismic waves and stated that their results suggest a lithosphere-atmosphere-ionosphere coupling.

With respect to EM induction studies, Padilha et al. (2017) published results on the effect of a huge crustal conductivity anomaly on the *H* component of geomagnetic variations recorded in central South America. These effects directly affect the geomagnetic records of our CBA station. They mixed the data collected by the Embrace MagNet with data from other observatories and temporary stations to report anomalous amplifications in the *H* component of the geomagnetic field. Such amplifications were explained on the basis of two phenomena of classical electrodynamics: reflection of EM waves at the interface with a very good conductor and the damping of the EM wave amplitude by the skin effect during its propagation through a conductive medium. In both abovementioned studies, the authors used the Embrace MagNet data with 1 s resolution to get to their conclusion.

3. Concluding Remarks

After the rise of a new fluxgate magnetometer network we presented a series of scientific findings along with recent publication based on the data collected by the Embrace MagNet to support that it is able to provide results that are comparable to the absolute measurement made at magnetic observatories, which are suitable for space weather studies.

With respect to the diurnal variation of monthly QDC measured at the Embrace MagNet stations, we identified that the changes in the solar activities cannot completely explain the different decreases observed from 2002 to 2012 in the daily variation over SLZ and EUS. This is attributed to the westward drift of the main magnetic field, which in turn is evidence that SLZ is no longer an equatorial station since circa 2012. It also means that another approach besides the “conversion table subdivided by seasonal,” once the data collected by the Embrace MagNet aimed to be used for deriving the K_sa index. Based on the QDC colored maps that show their evolution from September 2010 to March 2016 at 10 Embrace MagNet stations, we were also able to

Acknowledgments

C. M. Denardini thanks CNPq/MCTIC (grant 303121/2014-9), FAPESP (grant 2012/08445-9), and the Brazilian Government (Program 2056, Budget Action N387, and Budget Plan 08/2013–2017), which supported both the scientific and infrastructure projects that gave birth to the Embrace Magnetometer Network. S. S. Chen thanks CNPq/MCTIC (grant 134151/2017-8). L. C. A. Resende thanks CNPq/MCTIC (grant 405334/2017-6) and FAPESP (grant 2014/11198-9). J. Moro thanks China-Brazil Joint Laboratory for Space Weather and Chinese Academy of Science. N. J. Schuch thanks CNPq/MCTIC (grant 300886/2016-0, PQ-1D). A. V. Bilibio thanks CNPq/MCTIC (grant 143044/2017-6). P. R. Fagundes thanks FAPESP (grant 2012/08445-9), FINEP (grant 01.100661-00), and CNPq/MCTIC (grant 302927/2013-1). M. A. Gende thanks Agencia Nacional de Promoción Científica y Tecnológica-ANPCyT (grant PICT-2014-2301). M. A. Cabrera thanks FONCyT-MINCYT (grant BID-PICT 2015/0511) and UNT (grant PIUNT 26/E508) Argentina. M. J. A. Bolzan thanks CNPq/MCTIC (grant 301457/2009-3) and FAPEG (contract 2012.1026.7000905). A. L. Padilha thanks CNPq/MCTIC (grant 304353/2013-2). J. L. Hormaechea thanks UNLP and CONICET. P. F. Barbosa Neto thanks CAPES/MEC (grant 1622967). G. A. S. Picanço thanks CNPq/MCTIC (grant 830967/1999-0). T. O. Bertolotto thanks CNPq/MCTIC (grant 800012/2016-0). All the authors thank Embrace/INPE for providing the collected from the Embrace MagNet (<http://www.inpe.br/spaceweather>), Intermagnet for data collected at magnetic observatories, World Data Center for Geomagnetism at Kyoto (Japan) for the definitive Dst and Kp indices data, International Service of Geomagnetic Indices (ISGI) for the SSC and SI precise information, NOAA-NASA teams for X-ray flux from GOES 15 satellite, and WIND spacecraft data team for IMF Bz and solar wind parameters data. We also would especially thank the following persons and their corresponding institutions for kindly supporting the installation, maintenance, and operation of the Embrace MagNet Sensor at their facilities: Katia Jasbinschek dos Reis Pinheiro (Observatório Nacional, and Magnetic Observatory of Vassouras, MCTIC); Gerardo C. Connon, Carlos A. Ferrer (EARG, CONICET), and Luis H. Barbero (EARG, UNLP); Fernando Miranda Bonomi, Mariano Fagre, Luis Scidá, Rodolfo Ezquer, Pablo Bedoian, Graciela Molina (Facultad de Ciencias Exactas y Tecnología, UNT), and Guillermo Aceñolaza (Instituto Superior de Correlación Geológica, CONICET);

identify the diurnal and the seasonal variations, that is, 2 out of the 10 natural variations of the H component described in the literature.

When analyzing the response of the Embrace MagNet to the space weather drivers such as CME and HSS in terms of SSC and SI, we verified that the time of the SSC registered measured by the H component on the Embrace MagNet on 8 March 2012 matches with the SSC precise information revealed by the ISGI (which is essentially based on Intermagnet data). We also show that our measurements are consistent with the order of increases in IMF Bz and P_{sw} as well as its time lag between events. We attributed the measured SSC to the CME that hit the Earth on 8 March 2012. With respect to the SI chosen to exemplify the capability of the Embrace MagNet, it also matched in time information revealed by the ISGI and with other study published in the literature. In addition, we attributed its cause to a HSS arriving from the recurrent coronal hole that was passing close to the solar central meridian in the same period. In order to support that, we mentioned and discussed about the Alfvén waves present in the solar wind dynamic pressure prior and during the event.

The analysis of the response of the evolution of ΔH derived from the Embrace MagNet during the intense magnetic storm occurred on 12 October 2016 showed that our measurements provide excellent agreement with the Dst evolution, especially with respect to the timing of the magnetic storm and to the evolution of its phases. We also showed that there is a good agreement with respect to the ΔH amplitudes and the Dst, despite that the low-latitude stations of the South American sector registered a little higher value. The highlighted item was the fact that the Embrace MagNet station situated under the SAMA, that is, SMS, registered the highest variation of the H component.

The Embrace MagNet measurements were presented as a significant tool to investigate the effects of the Sq systems response to the X-class solar flares occurring during daytime under magnetically quiet conditions. The ΔH variation displayed simultaneous response throughout the entire network of stations. The low-latitude stations presented sudden positive impulses, while midlatitude station presented negative response. Very small amplitude oscillations in the magnetic measurement were also observed after the pick of the flare.

In addition to the scientific findings presented by the present authors, the magnetic data collected by the Embrace MagNet have been used to support studies on seismology, magnetotelluric, ionosphere, and its coupling with the neutral atmosphere. In general, data with 1 min resolution have been enough for the ionospheric studies. However, in order to use magnetic data to support seismological or magnetotelluric methods, data with 1 s time resolution will be required.

Finally, we would like to remark that several stations are fully operational and we have shown samples of the capability of this new magnetic network. It is equally important to mention that its main goal is to provide data with quality suitable enough for space weather studies, including creating the South American K index (Ksa). Furthermore, the collected data are fully open and accessible in acknowledgment basis at the Embrace Program website (<http://www.inpe.br/spaceweather>).

References

- Alken, P., & Maus, S. (2007). Spatio-temporal characterization of the equatorial electrojet from CHAMP, Orsted, and SAC-C satellite magnetic measurements. *Journal of Geophysical Research*, *112*, A09305. <https://doi.org/10.1029/2007JA012524>
- Allen, C. W. (1944). Relation between magnetic storms and solar activity. *Monthly Notices of the Royal Astronomical Society*, *104*(1), 13–21. <https://doi.org/10.1093/mnras/104.1.13>
- Araki, T. (1994). A physical model of the geomagnetic sudden commencement. In M. J. Engebretson, K. Takahashi, & M. Scholer (Eds.), *Solar wind sources of magnetospheric ultra-low-frequency waves* (pp. 183–200). Washington, DC: American Geophysical Union. <https://doi.org/10.1029/GM081p0183>
- Chapman, S., & Bartels, J. (1940). *Geomagnetism* (Vol. 2). London: Oxford University Press.
- Curto, J. J., Araki, T., & Alberca, L. F. (2007). Evolution of the concept of sudden storm commencements and their operative identification. *Earth, Planets and Space*, *59*(11), 1–12. <https://doi.org/10.1186/BF03352059>
- de Jesus, R., Batista, I. S., de Abreu, A. J., Fagundes, P. R., Venkatesh, K., & Denardini, C. M. (2017). Observed effects in the equatorial and low-latitude ionosphere in the South American and African sectors during the 2012 minor sudden stratospheric warming. *Journal of Atmospheric and Solar - Terrestrial Physics*, *157*(Supplement C), 78–89. <https://doi.org/10.1016/j.jastp.2017.04.003>
- Denardini, C. M., Abdu, M. A., Aveiro, H. C., Resende, L. C. A., Almeida, P. D. S. C., Olívio, É. P. A., et al. (2009). Counter electrojet features in the Brazilian sector: Simultaneous observation by radar, digital sounder and magnetometers. *Annales Geophysicae*, *27*(4), 1593–1603. <https://doi.org/10.5194/angeo-27-1593-2009>
- Denardini, C. M., Chen, S. S., Resende, L. C. A., Moro, J., Bilibio, A. V., Fagundes, P. R., et al. (2018). The Embrace Magnetometer Network for South America: Network description and its qualification. *Radio Science*, *53*. <https://doi.org/10.1002/2017RS006477>

Alexandre Tardelli (IP&D, Univap);
 Thiago Oliveira Lima (Laboratório de
 Física Espacial, UFG-Campus Jataí);
 Newton Lima (Ionospheric Laboratory at
 the Centro Universitário Luterano de
 Manaus, ULBRA); and Francisco Vieira
 (Observatório de Física Espacial, IFTO-
 Campus Araguatins).

- Denardini, C. M., Dasso, S., & Gonzalez-Esparza, J. (2016a). A Review on space weather in Latin America. 2. The research networks ready for space weather. *Advances in Space Research*, 58(10), 1940–1959. <https://doi.org/10.1016/j.asr.2016.03.013>
- Denardini, C. M., Dasso, S., & Gonzalez-Esparza, J. (2016b). A Review on space weather in Latin America. 3. Development of space weather forecasting centers. *Advances in Space Research*, 58(10), 1960–1967. <https://doi.org/10.1016/j.asr.2016.03.011>
- Denardini, C. M., Resende, L. C. A., Moro, J., & Chen, S. S. (2016). Occurrence of the blanketing sporadic E layer during the recovery phase of the October 2003 superstorm. *Earth, Planets and Space*, 68(80), 1–9.
- Denardini, C. M., Rockenbach, M., Gende, M. A., Chen, S. S., Fagundes, P. R., Schuch, N. J., et al. (2015). The initial steps for developing the South American K index from the embrace magnetometer network. *Brazilian Geophysics of Journal*, 33(1), 79–88.
- Gloeckler, G., Balsiger, H., Bürgi, A., Bochsler, P., Fisk, L. A., Galvin, A. B., et al. (1995). The solar WIND and suprathermal ion composition investigation on the WIND spacecraft. *Space Science Reviews*, 71(1–4), 79–124. <https://doi.org/10.1007/BF00751327>
- Gold, T. (1953). Discussion of shock waves and rarefied gases. In J. C. van de Hulst & J. M. Burgers (Eds.), *Gas dynamics of cosmic clouds* (pp. 97–105). Amsterdam: North-Holland Co.
- Gold, T. (1962). Magnetic storm. *Space Science Reviews*, 1, 100–114. <https://doi.org/10.1007/BF00174637>
- Gonzalez, W. D., Joselyn, J. A., Kamide, Y., Kroehl, H. W., Rostoker, G., Tsurutani, B. T., & Vasyliunas, V. M. (1994). What is a geomagnetic storm? *Journal of Geophysical Research*, 99(A4), 5771–5792. <https://doi.org/10.1029/93JA02867>
- Gopalswamy, N. (2016). History and development of coronal mass ejections as a key player in solar terrestrial relationship. *Geoscience Letters*, 3(1), 8. <https://doi.org/10.1186/s40562-016-0039-2>
- Gopalswamy, N., Mäkelä, P., Xie, H., Akiyama, S., & Yashiro, S. (2009). CME interactions with coronal holes and their interplanetary consequences. *Journal of Geophysical Research*, 114, A00A22. <https://doi.org/10.1029/2008JA013686>
- Jayapal, R., Gopal, S., Anilkumar, C. P., & Venugopal, C. (2016). A regional geomagnetic model using Fourier analysis. *International Research Journal of Natural and Applied Sciences*, 3(1), 1–13.
- Klausner, V., Almeida, T., de Meneses, F. C., Kherani, E. A., Pillat, V. G., Muella, M. T. A. H., & Fagundes, P. R. (2017). First report on seismogenic magnetic disturbances over Brazilian sector. *Pure and Applied Geophysics*, 174(3), 737–745. <https://doi.org/10.1007/s00024-016-1455-0>
- Lepping, R. P., Acuña, M. H., Burlaga, L. F., Farrell, W. M., Slavin, J. A., Schatten, K. H., et al. (1995). The WIND magnetic field investigation. *Space Science Reviews*, 71(1–4), 207–229. <https://doi.org/10.1007/BF00751330>
- Lindzen, R. S., & Chapman, S. (1969). Atmospheric tides. *Space Science Reviews*, 10, 3–188.
- Maeda, K., & Kato, S. (1966). Electrodynamics of the ionosphere. *Space Science Reviews*, 5(1), 57–79.
- Matsushita, S. (1962). On geomagnetic sudden commencements, sudden impulses, and storm durations. *Journal of Geophysical Research*, 67(10), 3753–3777. <https://doi.org/10.1029/JZ067i010p03753>
- Matsushita, S. (1969). Dynamo currents, winds and electric fields. *Radio Science*, 4(9), 771–1969.
- Mayaud, P. N. (1977). Equatorial counter-electrojet—A review of its geomagnetic aspects. *Journal of Atmospheric and Terrestrial Physics*, 39(9–10), 1055–1070. [https://doi.org/10.1016/0021-9169\(77\)90014-9](https://doi.org/10.1016/0021-9169(77)90014-9)
- Maynard, N. C., & Cahill, L. J. Jr. (1965a). Measurements of the equatorial electrojet over India. *Journal of Geophysical Research*, 70(23), 5923–5936. <https://doi.org/10.1029/JZ070i023p05923>
- Maynard, N. C., & Cahill, L. J. Jr. (1965b). Preliminary results of the measurements of Sq currents and equatorial electrojet near Peru. *Journal of Geophysical Research*, 70(23), 5975–5977. <https://doi.org/10.1029/JZ070i023p05975>
- Morton, R. J., Tomczyk, S., & Pinto, R. (2015). Investigating Alfvénic wave propagation in coronal open-field regions. *Nature Communications*, 6(1), 7813. <https://doi.org/10.1038/ncomms8813>
- Nogueira, P. A. B., Souza, J. R., Abdu, M. A., Paes, R. R., Sousa Santos, J., Marques, M. S., et al. (2015). Modeling the equatorial and low-latitude ionospheric response to an intense X-class solar flare. *Journal of Geophysical Research: Space Physics*, 120, 3021–3032. <https://doi.org/10.1002/2014JA020823>
- Obayashi, T. (1964). The streaming of solar flare particles and plasma in interplanetary space. *Space Science Reviews*, 3(1), 79–108. <https://doi.org/10.1007/BF00226645>
- Ofman, L., & Davila, J. M. (1995). Alfvén wave heating of coronal holes and the relation to the high-speed solar wind. *Journal of Geophysical Research*, 100(A12), 23,413–23,425. <https://doi.org/10.1029/95JA02222>
- Ogilvie, K. W., Burlaga, L. F., & Wilkerson, T. D. (1968). Plasma observations on Explorer 34. *Journal of Geophysical Research*, 73(21), 6809–6824. <https://doi.org/10.1029/JA073i021p06809>
- Ogilvie, K. W., Chornay, D. J., Fritzenreiter, R. J., Hunsaker, F., Keller, J., Lobell, J., et al. (1995). SWE, a comprehensive plasma instrument for the Wind spacecraft. *Space Science Reviews*, 71(1–4), 55–77. <https://doi.org/10.1007/BF00751326>
- Ouadfeul, S., Tourtchine, V., & Aliouane, L. (2015). Daily geomagnetic field prediction of INTERMAGNET observatories data using the multilayer perceptron neural network. *Arabian Journal of Geosciences*, 8(3), 1223–1227. <https://doi.org/10.1007/s12517-014-1308-z>
- Padilha, A. L., Alves, L. R., Silva, G. B. D., & Espinosa, K. V. (2017). Effect of a huge crustal conductivity anomaly on the H-component of geomagnetic variations recorded in central South America. *Earth, Planets and Space*, 69(1), 58. <https://doi.org/10.1186/s40623-017-0644-0>
- Rostoker, G. (1972). Geomagnetic indexes. *Reviews of Geophysics and Space Physics*, 10(4), 935–951. <https://doi.org/10.1029/RG010i004p0935>
- Samson, J. C. (1991). Geomagnetic pulsations and plasma waves in the Earth’s magnetosphere. In J. A. Jacobs (Ed.), *Geomagnetism* (Vol. 4, pp. 481–592). London: Academic Press.
- Samsonov, A. A., Sibeck, D. G., Walsh, B. M., & Zolotova, N. V. (2014). Sudden impulse observations in the dayside magnetosphere by THEMIS. *Journal of Geophysical Research: Space Physics*, 119, 9476–9496. <https://doi.org/10.1002/2014JA020012>
- Santos, A. M., Abdu, M. A., Souza, J. R., Sobral, J. H. A., Batista, I. S., & Denardini, C. M. (2016). Storm time equatorial plasma bubble zonal drift reversal due to disturbance Hall electric field over the Brazilian region. *Journal of Geophysical Research: Space Physics*, 121, 5594–5612. <https://doi.org/10.1002/2015JA022179>
- Schrijver, C. J., Kauristie, K., Aylward, A. D., Denardini, C. M., Gibson, S. E., Glover, A., et al. (2015). Understanding space weather to shield society: A global road map for 2015–2025 commissioned by COSPAR and ILWS. *Advances in Space Research*, 55(12), 2745–2807. <https://doi.org/10.1016/j.asr.2015.03.023>
- Schulte in den Bäumen, H., Moran, D., Lenzen, M., Cairns, I., & Steenge, A. (2014). How severe space weather can disrupt global supply chains. *Natural Hazards and Earth System Sciences*, 14(10), 2749–2759. <https://doi.org/10.5194/nhess-14-2749-2014>
- Schutz, S., Adams, G. J., & Mozer, F. S. (1974). Electric and magnetic fields measured during a sudden impulse. *Journal of Geophysical Research*, 79(13), 2002–2004. <https://doi.org/10.1029/JA079i013p02002>
- Shinbori, A., Nishimura, Y., Tsuji, Y., Kikuchi, T., Araki, T., Ikeda, A., et al. (2010). Anomalous occurrence features of the preliminary impulse of geomagnetic sudden commencement in the South Atlantic Anomaly region. *Journal of Geophysical Research*, 115, A08309. <https://doi.org/10.1029/2009JA015035>

- Siscoe, G. L., Formisano, V., & Lazarus, A. J. (1968). Relation between geomagnetic sudden impulses and solar wind pressure changes—An experimental investigation. *Journal of Geophysical Research*, *73*(15), 4869–4874. <https://doi.org/10.1029/JA073i015p04869>
- Sugiura, M., & Cain, J. C. (1966). A model equatorial electrojet. *Journal of Geophysical Research*, *71*(7), 1869–1877. <https://doi.org/10.1029/JZ071i007p01869>
- Sutcliffe, P. R. (1999). The development of a regional geomagnetic daily variation model using neural networks. *Annales Geophysicae*, *18*(1), 120–128. <https://doi.org/10.1007/s00585-000-0120-0>
- Thomson, N. R., Rodger, C. J., & Dowden, R. L. (2004). Ionosphere gives size of greatest solar flare. *Geophysical Research Letters*, *31*, L06803. <https://doi.org/10.1029/2003GL019345>
- Tsurutani, B. T., Echer, E., Shibata, K., Verkhoglyadova, O. P., Mannucci, A. J., Gonzalez, W. D., et al. (2014). The interplanetary causes of geomagnetic activity during the 7–17 March 2012 interval: A CAWSES II overview. *Journal of Space Weather and Space Climate*, *4*, A02. <https://doi.org/10.1051/swsc/2013056>
- Unnikrishnan, K. (2012). Artificial neural network (ANN) for modelling Earth's magnetic field belonging to solar minimum observed at a low latitude station Alibag. *Indian Journal of Radio & Space Physics*, *41*(3), 359–366.
- Venkatesh, K., Fagundes, P. R., Prasad, D. S. V. V. D., Denardini, C. M., de Abreu, A. J., de Jesus, R., & Gende, M. (2015). Day-to-day variability of equatorial electrojet and its role on the day-to-day characteristics of the equatorial ionization anomaly over the Indian and Brazilian sectors. *Journal of Geophysical Research: Space Physics*, *120*, 9117–9131. <https://doi.org/10.1002/2015JA021307>
- Vestine, E. H. (1960). The upper atmosphere and geomagnetism. In J. A. Ratcliffe (Ed.), *Physics of the upper atmosphere* (pp. 471–512). New York: Academic Press.
- Vestine, E. H., Laporte, L., Lange, I., & Scott, W. E. (1947). *The geomagnetic field, its description and analysis* (1st ed.). Washington, DC: Carnegie Institution of Washington Publication.
- Wilson, L. B., Cattell, C., Kellogg, P. J., Goetz, K., Kersten, K., Hanson, L., et al. (2007). Waves in interplanetary shocks: A Wind/WAVES study. *Physical Review Letters*, *99*(4), 41101. <https://doi.org/10.1103/PhysRevLett.99.041101>